Supporting Information

Shifting the Equilibrium between the Encounter State and the Specific Form of a Protein Complex by Interfacial Point Mutations

Alexander N. Volkov, Qamar Bashir, Jonathan A. R. Worrall, G. Matthias Ullmann, and Marcellus Ubbink

Theory

Decomposition of the free binding energy into the contributions of the specific and encounter forms. Cc and CcP form a complex <Cc:CcP> with a degenerate energy level consisting of two sub-levels: those of a specific form Cc:CcP and an encounter state $(Cc:CcP)^*$. Complex formation can be described by the scheme 1:

$$Cc + CcP \rightleftharpoons <Cc:CcP> \quad (1)$$

with the equilibrium constant (K_0) given by

$$K_0 = \frac{a(\langle Cc:CcP\rangle)}{a(Cc)a(CcP)} = \frac{[\langle Cc:CcP\rangle]}{[Cc][CcP]} \times \frac{\gamma(\langle Cc:CcP\rangle)}{\gamma(Cc)\gamma(CcP)} \approx \frac{[\langle Cc:CcP\rangle]}{[Cc][CcP]} \quad (2)$$

where a and γ are activities and activity coefficients, respectively. In dilute protein solutions used in this study, the latter approach 1 M^{-1} (ref 1). Note that K_0 and other equilibrium constants defined below are dimensionless entities. The populations of the free proteins (P_0) and the <Cc:CcP> complex (P_1) in scheme 1 are:

$$P_0 = \frac{1}{1+2K_0} \qquad P_1 = \frac{2K_0}{1+2K_0} \quad (3)$$

where factor 2 in $2K_0$ term reflects the two-fold degeneracy of the energy level[1].

Formation of the specific form and the encounter state can be described by the scheme 4:

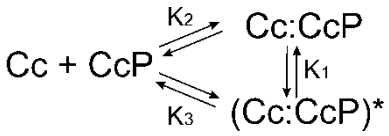

(4)

where the corresponding equilibrium constants and populations of the free proteins (P_0), the specific form (P_2), and the encounter state (P_3) are given by

$$K_1 = \frac{[Cc:CcP]}{[(Cc:CcP)^*]} \qquad K_2 = \frac{[Cc:CcP]}{[Cc][CcP]} \qquad K_3 = \frac{[(Cc:CcP)^*]}{[Cc][CcP]} \quad (5)$$

$$P_0 = \frac{1}{1+K_2+K_3} \qquad P_2 = \frac{K_2}{1+K_2+K_3} \qquad P_3 = \frac{K_3}{1+K_2+K_3} \quad (6)$$

Equating P_0 terms from (eq 3) and (eq 6), and noting that $K_1 = K_2/K_3$, yields $K_2 = 2K_0K_1/(1 + K_1)$ and $K_3 = 2K_0/(1 + K_1)$. Finally, using the experimental free binding energy for <Cc:CcP> (ΔG_0) and the population of the encounter state (p) derived from PRE NMR and given by eq 7

$$p = \frac{[(Cc:CcP)^*]}{[Cc:CcP]+[(Cc:CcP)^*]} = \frac{1}{K_1+1} \quad (7)$$

allows to derive the free energy contributions of the specific form (ΔG_2) and the encounter state (ΔG_3):

$$\Delta G_2 = -RT\ln(K_2) = -RT\ln\left(\frac{2K_0K_1}{1+K_1}\right) = \Delta G_0 + RT\ln\left(\frac{1+K_1}{2K_1}\right) = \Delta G_0 - RT\ln(2(1-p)) \quad (8)$$

$$\Delta G_3 = -RT\ln(K_3) = -RT\ln\left(\frac{2K_0}{1+K_1}\right) = \Delta G_0 + RT\ln\left(\frac{1+K_1}{2}\right) = \Delta G_0 - RT\ln(2p) \quad (9)$$

The errors in ΔG_2 and ΔG_3 are propagated from the uncertainties in ΔG_0 and p as

$$\delta(\Delta G_2) = \sqrt{\delta^2(\Delta G_0) + (RT\delta(p)/(1-p))^2} \text{ and } \delta(\Delta G_3) = \sqrt{\delta^2(\Delta G_0) + (RT\delta(p)/p)^2} \quad (10)$$

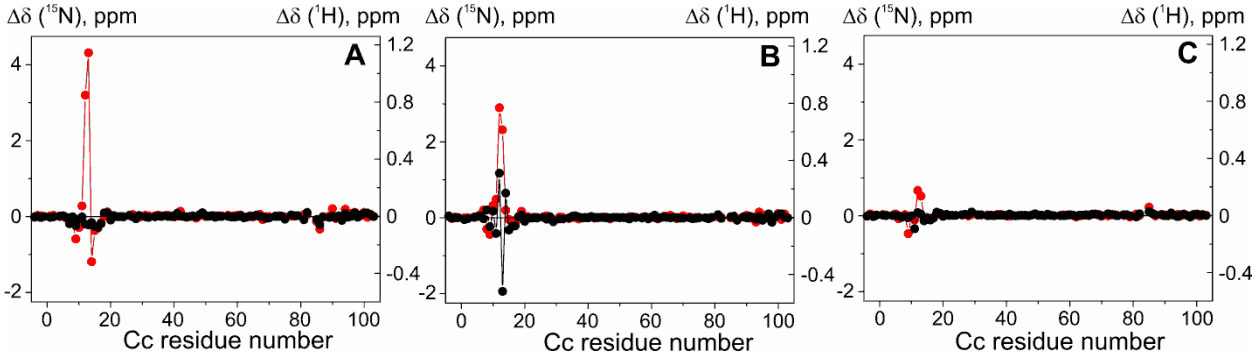

Figure S1. Effects of mutations on the chemical shifts of Cc backbone amides. Changes in the chemical shifts (Δδ) of backbone amide nitrogens (red circles) and protons (black circles) for (A) R13A, (B) T12A, and (C) R13K Cc, relative to those of wt Cc.

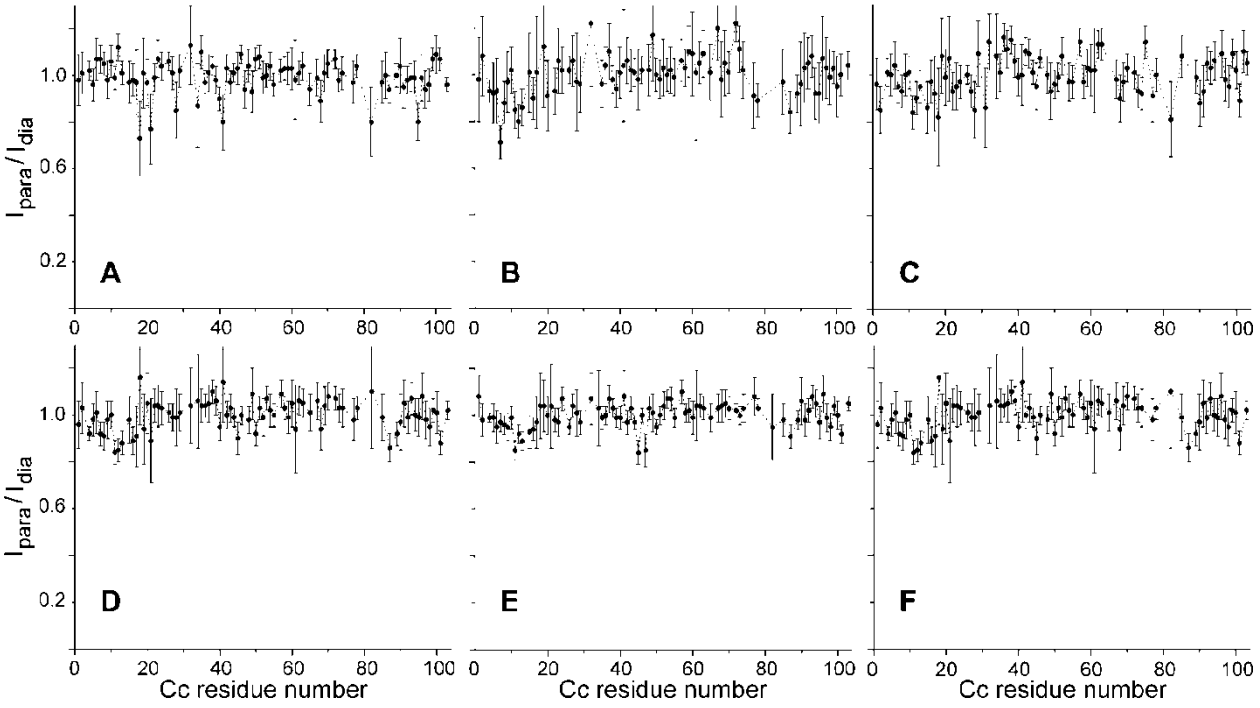

Figure S2. Paramagnetic effects in R13A Cc - CcP-SL complexes. Relative [^{1}H, ^{15}N] HSQC intensities of Cc backbone amides in the complex with CcP labeled with a paramagnetic SL (I_{para}) or a diamagnetic analogue (I_{dia}) at positions (A) V10C, (B) K97C, (C) T137C, (D) N141C, (E) N164C, and (F) L213C. The error bars denote standard deviations, derived from spectral noise levels using standard error propagation procedures.

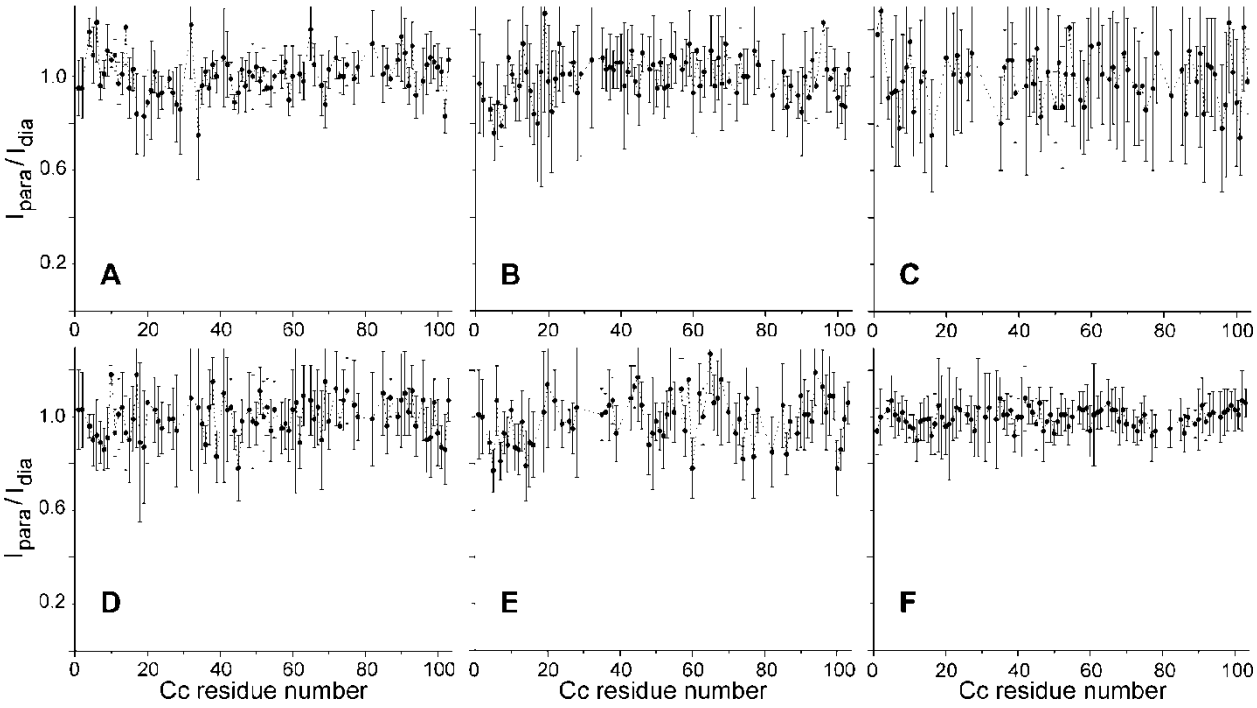

Figure S3. Paramagnetic effects in R13K Cc - CcP-SL complexes. Relative [^{1}H, ^{15}N] HSQC intensities of Cc backbone amides in the complex with CcP labeled with a paramagnetic SL (I_{para}) or a diamagnetic analogue (I_{dia}) at positions (A) V10C, (B) K97C, (C) N141C, (D) N164C, (E) L213C, and (F) S263C. The error bars denote standard deviations, derived from spectral noise levels using standard error propagation procedures.

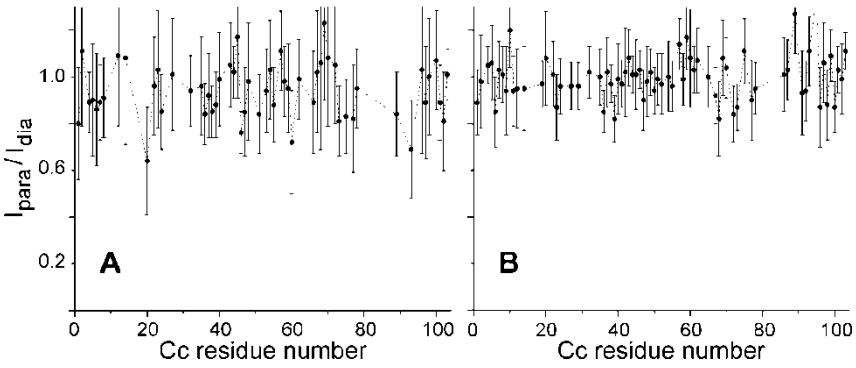

Figure S4. Paramagnetic effects in T12A Cc - CcP-SL complexes. Relative [^{1}H, ^{15}N] HSQC intensities of Cc backbone amides in the complex with CcP labeled with a paramagnetic SL (I_{para}) or a diamagnetic analogue (I_{dia}) at positions (A) T137C, and (B) S263C. The error bars denote standard deviations, derived from spectral noise levels using standard error propagation procedures.

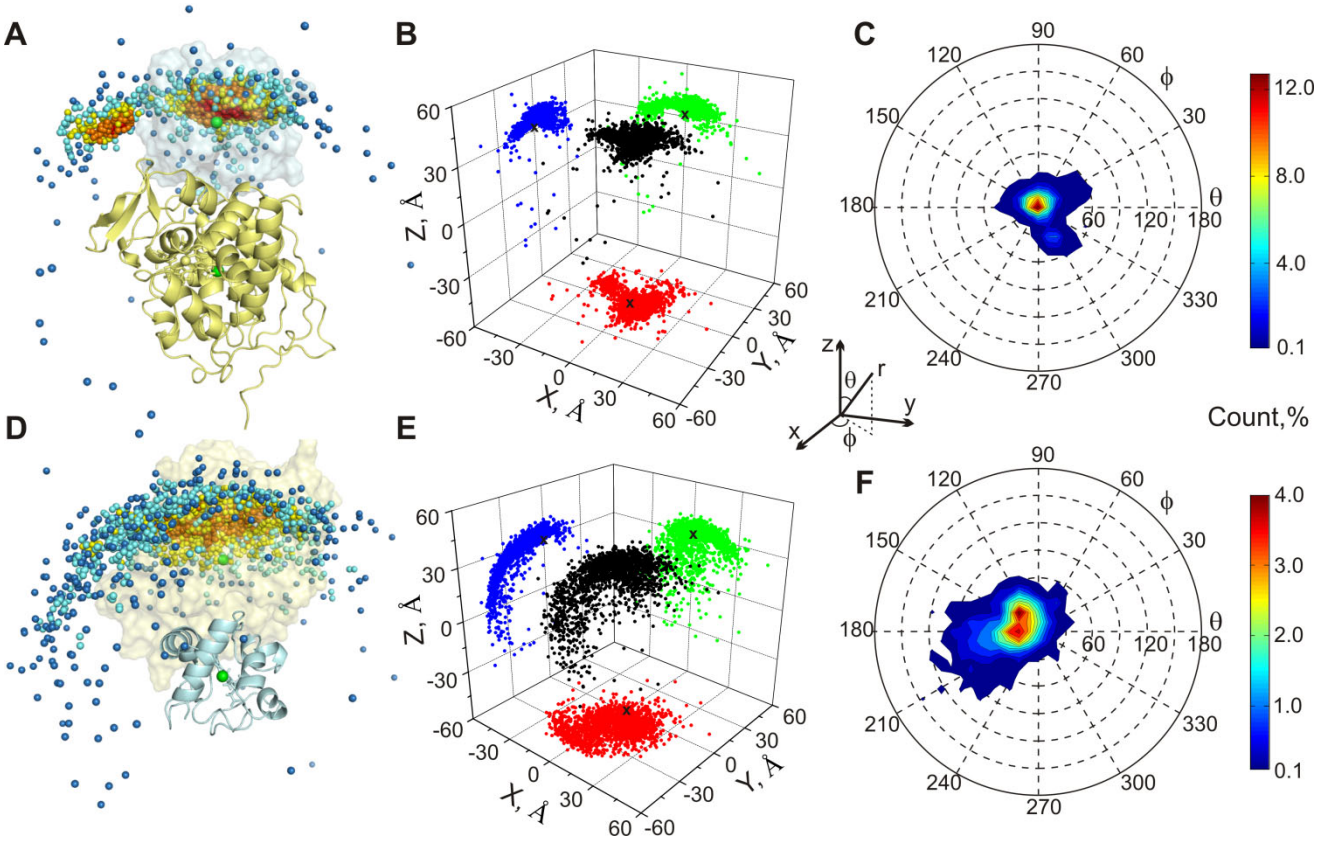

Figure S5. Monte Carlo simulation of wt Cc - CcP encounter state. (A, D) Spatial distribution of the encounter complexes and the distribution of the centers mass of (A-C) Cc around CcP and (D-F) CcP around Cc in (B, E) Cartesian and (C, F) spherical coordinate systems. See the legend to main-text Figure 7 for details.

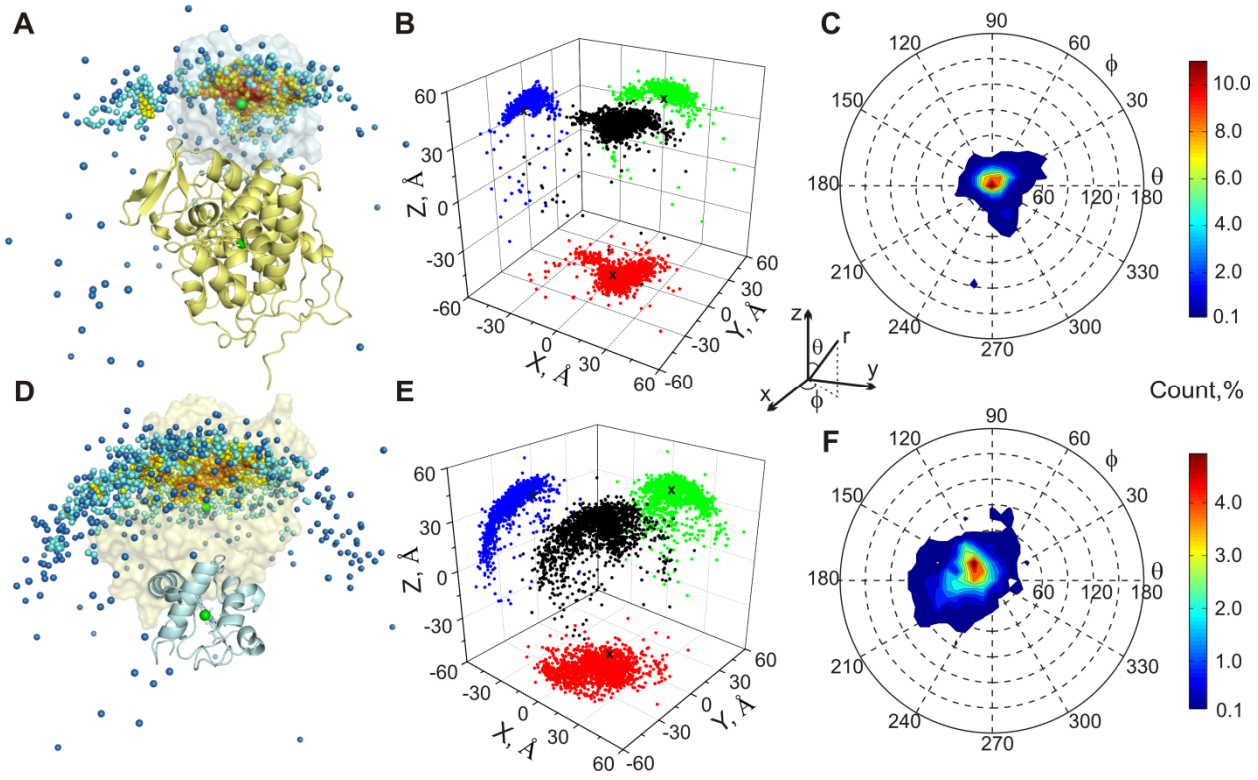

Figure S6. Monte Carlo simulation of R13K Cc - CcP encounter state. (A, D) Spatial distribution of the encounter complexes and the distribution of the centers mass of (A-C) Cc around CcP and (D-F) CcP around Cc in (B, E) Cartesian and (C, F) spherical coordinate systems. See the legend to main-text Figure 7 for details.

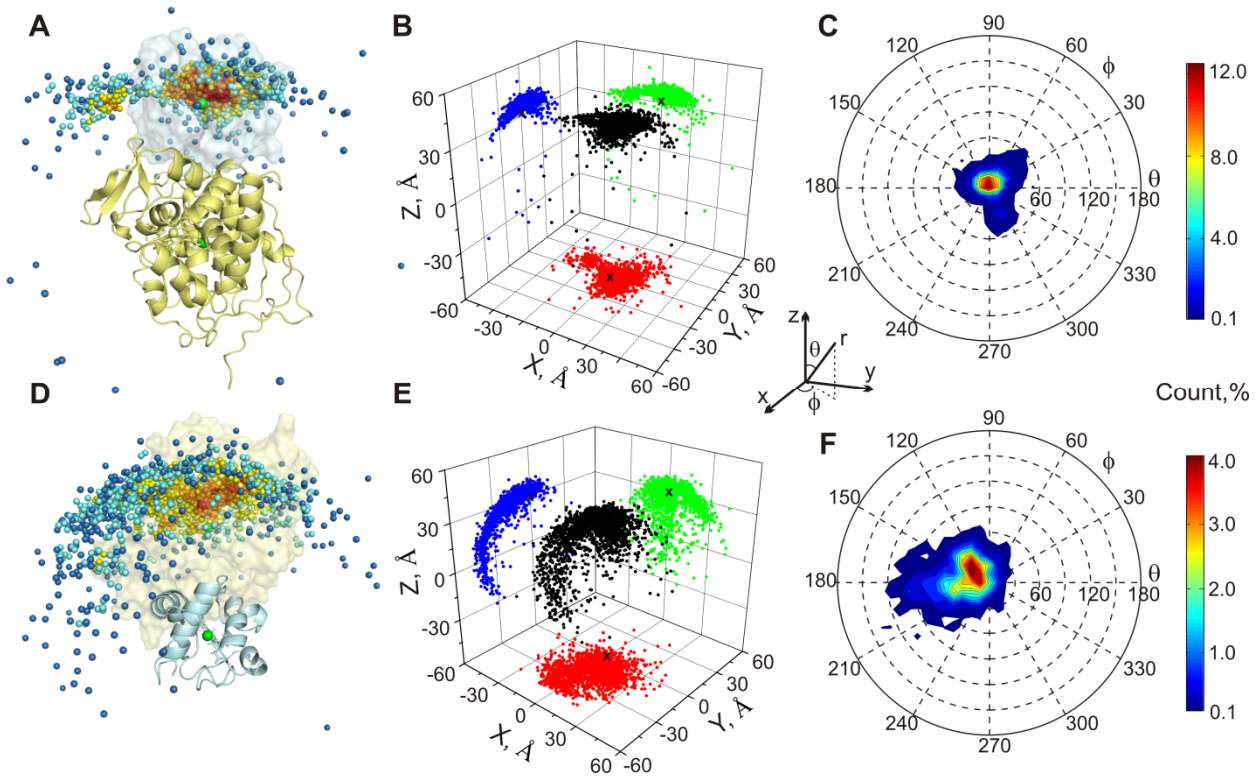

Figure S7. Monte Carlo simulation of T12A Cc - CcP encounter state. (A, D) Spatial distribution of the encounter complexes and the distribution of the centers mass of (A-C) Cc around CcP and (D-F) CcP around Cc in (B, E) Cartesian and (C, F) spherical coordinate systems. See the legend to main-text Figure 7 for details.

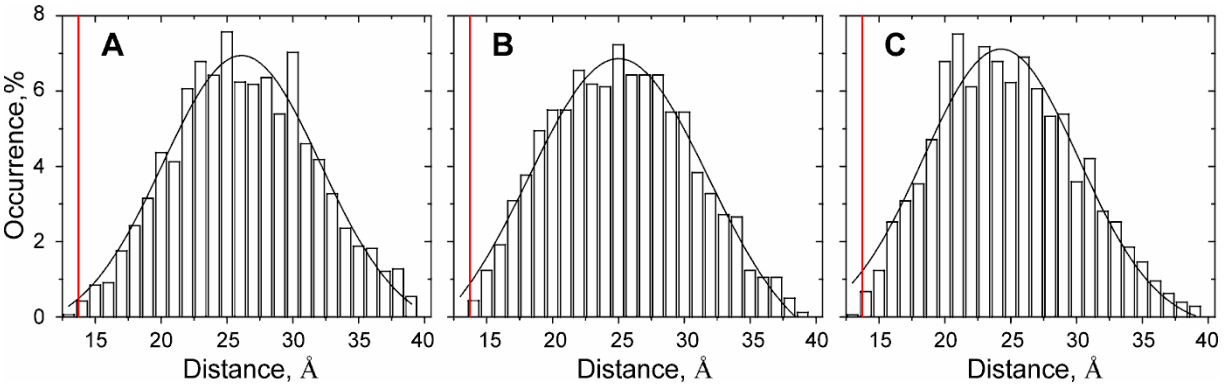

Figure S8. Intermolecular ET donor-acceptor distances in the encounter state. Edge-to-edge distances between the aromatic ring of CcP W191[2,3] and heme group of Cc in the simulated encounter ensembles of (*A*) R13A, (*B*) R13K, and (*C*) T12A Cc - CcP. Black lines are Gaussian fits of the distributions with parameters (A) $r^2 = 0.95$ and $x_c = 26.1 \pm 0.2$ Å; (B) $r^2 = 0.97$, $x_c = 25.0 \pm 0.2$ Å; and (C) $r^2 = 0.95$, $x_c = 24.3 \pm 0.2$ Å. The red line marks the distance in the specific complex (13.7 Å).

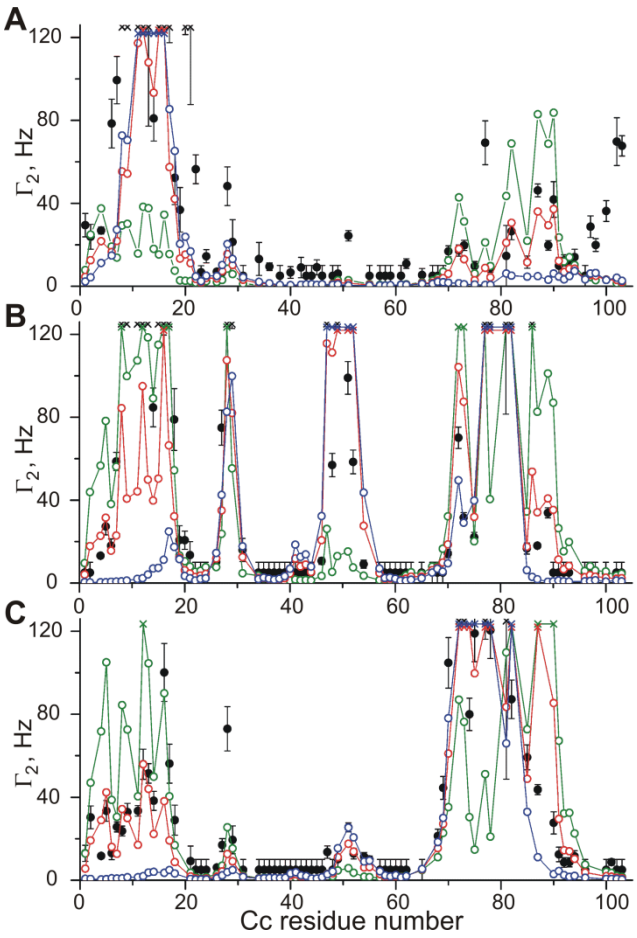

Figure S9. Observed and calculated PREs for R13K Cc - CcP-SL complexes. PRE profiles for SLs attached at position (*A*) N38C, (*B*) N200C and (*C*) T288C. Experimental Γ_2^{obs} (black) and PREs back-calculated for the specific orientation (blue), simulated encounter state (green), and the combination of the two (red) at the optimal p value of 0.4. See the legend to main-text Figure 9 for more details.

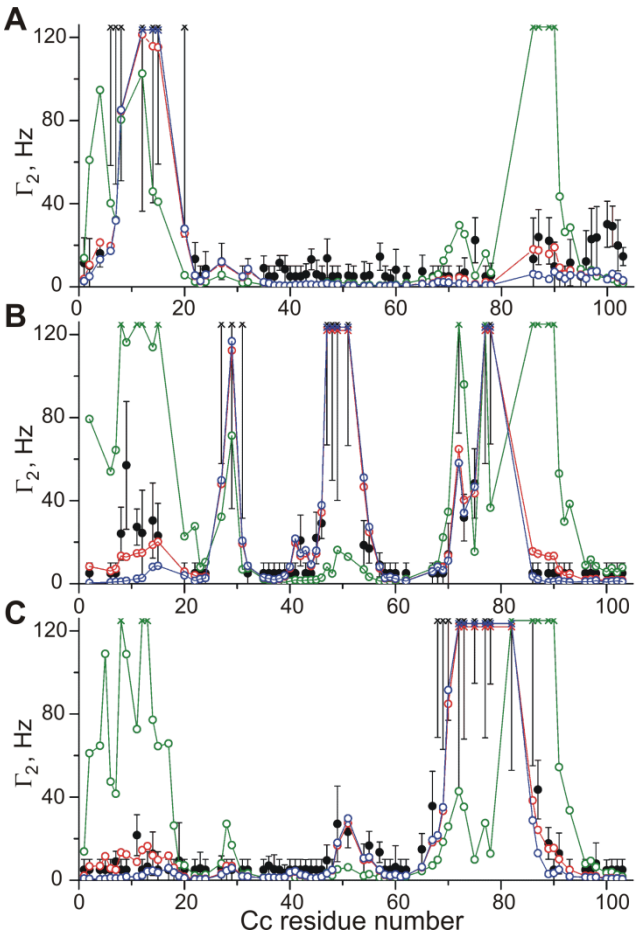

Figure S10. Observed and calculated PREs for T12A Cc - CcP-SL complexes. PRE profiles for SLs attached at position (*A*) N38C, (*B*) N200C and (*C*) T288C. Experimental Γ_2^{obs} (black) and PREs back-calculated for the specific orientation (blue), simulated encounter state (green), and the combination of the two (red) at the optimal p value of 0.1. See the legend to main-text Figure 9 for more details.

Reference 46

MacKerell, A. D.; Bashford, D.; Bellott; Dunbrack, R. L.; Evanseck, J. D.; Field, M. J.; Fischer, S.; Gao, J.; Guo, H.; Ha, S.; Joseph-McCarthy, D.; Kuchnir, L.; Kuczera, K.; Lau, F. T. K.; Mattos, C.; Michnick, S.; Ngo, T.; Nguyen, D. T.; Prodhom, B.; Reiher, W. E.; Roux, B.; Schlenkrich, M.; Smith, J. C.; Stote, R.; Straub, J.; Watanabe, M.; Wiorkiewicz-Kuczera, J.; Yin, D.; Karplus, M. *J. Phys. Chem. B* **1998**, *102*, 3586-3616.

Supplementary References

(1) Atkins, P.; De Paula, J. *Atkins' Physical Chemistry*; Oxford University Press: Oxford, 2006; pp 796-802.

(2) Miller, M. A.; Vitello, L. B.; Erman, J. E. *Biochemistry* **1995**, *34*, 12048-12058.

(3) Hays Putnam, A. M.; Lee, Y. T.; Goodin, D. B. *Biochemistry* **2009**, *48*, 1-3.